

Mitochondrial respiratory chain-dependent generation of superoxide anion and its release into the intermembrane space

Derick HAN, Everett WILLIAMS and Enrique CADENAS¹

Department of Molecular Pharmacology and Toxicology, School of Pharmacy, University of Southern California, 1985 Zonal Avenue, Los Angeles, CA 90089-9121, U.S.A.

It has been generally accepted that superoxide anion generated by the mitochondrial respiratory transport chain are vectorially released into the mitochondrial matrix, where they are converted to hydrogen peroxide through the catalytic action of Mn-superoxide dismutase. Release of superoxide anion into the intermembrane space is a controversial topic, partly unresolved by the reaction of superoxide anion with cytochrome *c*, which faces the intermembrane space and is present in this compartment at a high concentration. This study was aimed at assessing the topological site(s) of release of superoxide anion during respiratory chain activity. To address this issue, mitoplasts were prepared from isolated mitochondria by digitonin treatment to remove portions of the outer membrane along with portions of cytochrome *c*. EPR analysis in conjunction with spin traps of antimycin-supplemented mitoplasts revealed the formation of a spin adduct of superoxide anion. The EPR signal was (i) abrogated by superoxide dismutase, (ii) decreased competitively by exogenous ferricytochrome *c* and (iii) broadened by the

membrane-impermeable spin-broadening agent chromium trioxalate. These results confirm the production and release of superoxide anion towards the cytosolic side of the inner mitochondrial membrane. In addition, co-treatment of mitoplasts with myxothiazol and antimycin A, resulting in an inhibition of the oxidation of ubiquinol to ubisemiquinone, abolished the EPR signal, thus suggesting that ubisemiquinone autoxidation at the outer site of the complex-III ubiquinone pool is a pathway for superoxide anion formation and subsequent release into the intermembrane space. The generation of superoxide anion towards the intermembrane space requires consideration of the mitochondrial steady-state values for superoxide anion and hydrogen peroxide, the decay pathways of these oxidants in this compartment and the implications of these processes for cytosolic events.

Key words: antimycin A, cytochrome *c*, hydrogen peroxide, superoxide dismutase, ubiquinone pool.

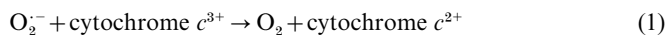
INTRODUCTION

Mitochondria from various aerobic organisms have been recognized as effective sources of H₂O₂ [1], a species that plays prominent roles in diverse pathophysiological processes, such as neurodegeneration, aging, and heart and lung toxicity. The production of H₂O₂ by mitochondria appears to account for 1–2% of the total O₂ consumed *in vitro* [1]. The superoxide anion radical (O₂^{•-}), formed during ubisemiquinone autoxidation and, secondarily, NADH dehydrogenase activity, is considered the stoichiometric precursor of mitochondrial H₂O₂ [1–7].

O₂^{•-}, generated during transfer of electrons through the respiratory chain, was proposed to be vectorially released into the mitochondrial matrix, where it becomes a substrate for Mn-superoxide dismutase. This view has been supported by the following observations: (i) the mitochondrial matrix contains high levels of Mn-superoxide dismutase (1.1 × 10⁻⁵ M) [8] and, expectedly, the high rate of O₂^{•-} production in the mitochondrial inner membrane would have a functional relationship with the localization of this enzyme; (ii) submitochondrial particles, where the inner membrane is inverted, generate O₂^{•-} into the medium as monitored by cytochrome *c*- [4] or adrenaline-based assays [3] and (iii) H₂O₂, the product of O₂^{•-} dismutation, is readily measured diffusing out from mitochondria by peroxidase-based assays [1]. Hence, the notion that H₂O₂ released by mitochondria is the product of dismutation of O₂^{•-} within the mitochondrial matrix has generally been accepted.

The topology of complex III (*bc*₁ complex) in the mitochondrial electron-transport chain involves an inner (UQ_i) and outer

(UQ_o) pool of ubiquinone (UQ), facing the matrix and the intermembrane space, respectively. Ubisemiquinone is formed at both the UQ_i site that lies near the matrix and at the UQ_o site in the vicinity of the intermembrane space [9,10]. This, along with ubisemiquinone autoxidation as a major source of O₂^{•-} formation by mitochondria, suggests the possibility of a partial production and release of O₂^{•-} towards the intermembrane space. However, the environment of the intermembrane space renders detection of O₂^{•-} difficult because this space contains: (i) millimolar levels of ferricytochrome *c*, which reacts with O₂^{•-} at considerable rates (eqn. 1; $k_1 = 2.5 \times 10^5 \text{ M}^{-1} \cdot \text{s}^{-1}$) [11]:



and (ii) a Cu,Zn-superoxide dismutase isoform [8,12–14]; the occurrence of this enzyme in the intermembrane space was questioned and attributed to contamination with lysosomes [15] but, more recently, evidence for its localization in this compartment was brought forward [15a]. Although the function and concentration in the intermembrane space of the latter remains to be determined, a similar argument as that stated above may be advanced, i.e. that the level of O₂^{•-} in the intermembrane space has a functional relationship with the localization of Cu,Zn-superoxide dismutase in this compartment.

This study was aimed at evaluating the topological site(s) of release of O₂^{•-} in mitochondria with experimental approaches involving mitoplasts (devoid of portions of the outer mitochondrial membrane) and the use of membrane-impermeable spin-broadening agents detected by EPR.

Abbreviations used: DMPO, 5,5'-dimethyl-1-pyrroline-*N*-oxide; TFA, thenoyltrifluoroacetone; UQ, ubiquinone; UQ_i, inner pool of UQ; UQ_o, outer pool of UQ.

¹ To whom correspondence should be addressed (e-mail cadenas@hsc.usc.edu).

MATERIALS AND METHODS

Chemicals and biochemicals

5,5'-Dimethyl-1-pyrroline-*N*-oxide (DMPO), Cu,Zn-superoxide dismutase, myxothiazol, ubiquinone-1 (UQ₁) and cytochrome *c* were obtained from Sigma (St. Louis, MO, U.S.A.). Chromium trioxalate and digitonin were purchased from Aldrich Chemicals (Milwaukee, WI, U.S.A.).

Isolation of mitochondria

Liver mitochondria were isolated from adult male Wistar rats by differential centrifugation as described previously [16]. Livers from rats were excised, washed with 0.25 M sucrose and homogenized in H medium (210 mM mannitol/70 M sucrose/2 mM Hepes/0.05% BSA). The homogenate was centrifuged at 800 *g* for 8 min, the pellet removed, and the centrifugation process repeated. The resulting supernatant was centrifuged at 8000 *g* for 10 min, washed with H medium and the centrifugation repeated.

Preparation of mitoplasts

Mitoplasts were prepared from isolated mitochondria by digitonin treatment as described previously [16]. Briefly, mitochondria (40 mg/ml) were mixed with an equal volume of H medium containing digitonin and stirred for 15 min on ice. The sample was diluted 6-fold with medium and centrifuged at 10000 *g* for 10 min. The pellet was washed once with H medium and the suspension centrifuged a final time (10000 *g* for 10 min).

Oxygen consumption

Oxygen uptake was measured polarographically with a Clark-type electrode (Hansatech, King's Lynn, Norfolk, U.K.). Mitochondrial and mitoplast respiration were determined in respiration buffer containing 230 mM mannitol, 70 mM sucrose, 30 mM Tris/HCl, 4 mM MgCl₂, 5 mM KH₂PO₄, 1 mM EDTA and 0.1% BSA, pH 7.4.

EPR

For EPR analysis, mitoplasts (1 mg) were placed in 200 μ l of buffer (230 mM mannitol/70 mM sucrose/20 mM Tris/HCl; pH adjusted to 7.4 with Mops) in the absence or presence of mitochondrial respiratory substrates or inhibitors. DMPO (160 mM) was added and the EPR spectra were recorded on a Bruker ECS106 spectrometer. Instrument settings were as follows: receiver gain, 5×10^4 ; microwave power, 20 mW; microwave frequency, 9.81 GHz; modulation amplitude, 0.505 G; time constant, 1.3 s; scan time, 167.7 s; scan width, 100 G. The EPR traces shown in the figures are summations of five scans.

Fumarase assay

Measurement of fumarase activity was determined as described previously [17].

RESULTS

Mitoplast functional integrity

Effect of digitonin on mitochondrial respiration

The outer mitochondrial membrane contains a higher level of cholesterol than the inner membrane and, hence, it is more susceptible to digitonin treatment [18]. Digitonin, in a dose-dependent manner, caused the loss of state-3 respiration (Figure 1), which was restored upon addition of exogenous cytochrome *c*, thus suggesting that the impairment of mitochondrial respiration

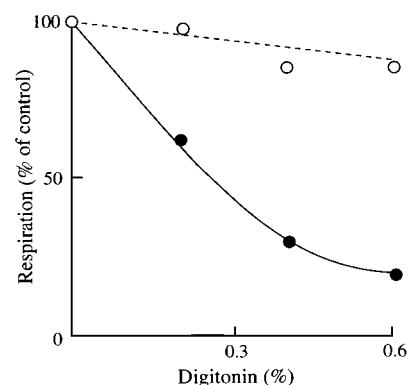


Figure 1 Effect of digitonin on mitochondrial respiration

Mitochondria (40 mg/ml) were treated with different digitonin concentrations for 15 min while stirring. Respiration (state 3) in the absence (●) or presence (○) of exogenous cytochrome *c* (2.5 μ M) was measured as described in the Materials and methods section. Respiration (%) = (mitoplast O₂ consumption/fumarase activity)/(mitochondrial O₂ consumption/fumarase activity). Fumarase activity was used instead of protein because mitochondrial purity was affected by digitonin treatment.

Table 1 Mitoplast and mitochondrial functional parameters

Isolation of mitochondria and mitoplasts and polarographic measurements were as described in the Materials and methods section. Measurements were performed with 7.5 mM succinate as an electron donor in the presence (state 3) or absence (state 4) of ADP. Where indicated, 2.5 μ M cytochrome *c* was added. States 3 and 4 are expressed in terms of ng of atoms of O/min per mg of protein (means \pm S.D., $n = 7$). The respiratory control ratio is defined as the state 3/state 4 ratio. ND, not determined.

	Mitochondria	Mitoplasts
State 3		
Control	41.7 \pm 20.3	25.9 \pm 16.4
+ Cytochrome <i>c</i>	42.3 \pm 18.5	41.9 \pm 23.4
State 4		
Control	8.95 \pm 4.9	10.9 \pm 6.7
+ Cytochrome <i>c</i>	ND	19.1 \pm 11.9
Respiratory control ratio		
Control	4.66 \pm 2.4	2.38 \pm 1.48
+ Cytochrome <i>c</i>	ND	2.19 \pm 1.29

after digitonin treatment was primarily due to a loss of this haemoprotein.

Mitoplast functional parameters

Digitonin is known to puncture holes in the outer membrane of mitochondria but at higher doses the functions of inner membrane are affected as well. Digitonin levels greater than 0.4% (w/v; at 40 mg/ml mitochondria) were highly effective in removing cytochrome *c* from the intermembrane space; however, this concentration resulted in uncoupling of oxidative phosphorylation (results not shown). At a digitonin concentration of 0.2%, mitoplasts remained coupled, despite the loss of a portion of cytochrome *c* (Table 1 and Figure 1). The functional parameters of mitoplasts generated by treatment of mitochondria with 0.2% digitonin are listed in Table 1. Overall, mitoplasts retained the respiratory parameters of mitochondria in the presence of exogenous cytochrome *c*, except for a drop in the respiratory control ratio that is usually observed with mitoplasts [19].

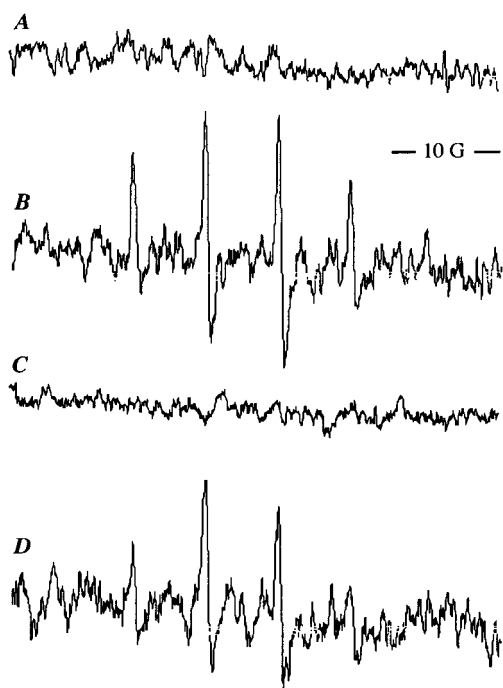


Figure 2 Formation of superoxide anion by mitoplasts

The reaction mixture consisted of mitoplasts (1 mg of protein/ml) in buffer (230 mM mannitol/70 mM sucrose/20 mM Tris/HCl, pH 7.4), supplemented with 160 mM DMPO and respiratory substrate and/or inhibitor. (A) Mitoplasts; (B) mitoplasts plus antimycin; (C) mitoplasts, antimycin and superoxide dismutase; (D) mitoplasts, antimycin and succinate. When present, the concentrations of succinate, antimycin and superoxide dismutase were 7.5 mM, 1 μ g/mg of protein and 400 units/ml, respectively.

Superoxide anion production by mitoplasts

Spin-trapping EPR of superoxide anion

Previous work with intact mitochondria and submitochondrial particles has established that production of $O_2^{\cdot-}$ and H_2O_2 increases substantially in the presence of antimycin [4], due to an increase in the steady-state levels of the ubisemiquinone pool caused by inhibition of electron transfer at the UQ_1 site in the Q-cycle. Likewise, antimycin was required to observe an EPR signal with mitoplasts respiring on endogenous substrates (Figure 2B); the EPR spectrum displayed the characteristics of a DMPO-OH adduct ($a^H = 14.9$; $a^N = 14.9$). Superoxide dismutase abolished the EPR signal (Figure 2C), thus suggesting that the DMPO-OH adduct originated from the spontaneous decay of a DMPO-superoxide adduct (DMPO-OOH) [20].

Stability of the DMPO spin adduct

As mentioned above, mitoplasts respiring on endogenous substrates generated an EPR signal ascribed to the $O_2^{\cdot-}$ spin adduct; the intensity of this signal (Figure 2B) was higher than that obtained in the presence of complex I or II respiratory substrates (e.g. succinate, Figure 2D). This discrepancy may be explained by considering that the electron-transport chain channels reducing equivalents on to the DMPO spin adducts, reducing them to EPR-silent hydroxylamines [21,22]. In agreement with this notion, mitoplasts supplemented with respiratory substrates decreased the intensity of a DMPO-OH adduct (generated by incubation of DMPO with H_2O_2 and Fe^{2+}) faster than mitoplasts respiring on endogenous substrates (Figure 3). The respiratory

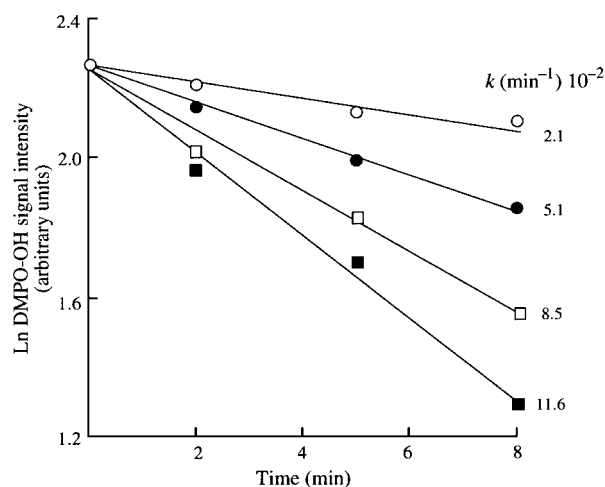


Figure 3 Effect of mitoplasts and respiratory substrates on the stability of the DMPO-OH spin adduct

The DMPO-OH adduct was generated upon incubation of 100 μ M H_2O_2 , 20 μ M ferrous ammonium sulphate and 100 mM DMPO for 2 min. Mitoplasts (0.2 mg of protein) with or without substrates were added and decay of the DMPO-OH signal monitored. \circ , No treatment; \bullet , mitoplasts plus antimycin; \square , mitoplasts, antimycin and succinate; \blacksquare , mitoplasts, antimycin and glutamate/pyruvate. Concentrations of reactants were 7.5 mM succinate, 7.5 mM malate/glutamate and 1 μ g of antimycin/mg of protein. Values represent first-order rate constants for the decay of the DMPO signal.

substrates themselves had no effect on DMPO-OH signal intensity (results not shown), suggesting that mitoplasts catalysed the reduction of the spin adduct at the expense of exogenous electron donors.

Localization of the EPR signal

Cu,Zn-superoxide dismutase, which cannot cross membranes, abolished the DMPO-OH signal originating from mitoplasts, thus suggesting that $O_2^{\cdot-}$ was released towards the intermembrane space. This notion was strengthened by two other experimental approaches: competition experiments involving cytochrome *c* and the use of the spin-broadening agent chromium trioxalate. Both cytochrome *c* and chromium trioxalate are membrane-impermeable probes; hence, their effects on the EPR signals (albeit by different mechanisms) are expected to take place on the cytosolic side of the inner membranes of mitoplasts.

The rate of reaction of $O_2^{\cdot-}$ with ferricytochrome *c* (eqn. 1; $k_1 = 2.5 \times 10^5 \text{ M}^{-1} \cdot \text{s}^{-1}$) [11] is faster than that with DMPO (eqn. 2; $k_2 = 10 \text{ M}^{-1} \cdot \text{s}^{-1}$) [20]:



Analysis of the competition between cytochrome *c* and $O_2^{\cdot-}$ requires consideration of the above rate constants and concentrations of reactants (e.g. $[\text{DMPO}] \gg [\text{cytochrome } c^{3+}]$). Addition of exogenous ferricytochrome *c* to antimycin-treated mitoplasts inhibited the DMPO-OH signal in a dose-dependent manner and in agreement with eqn. (3) (see Figure 4 for comparison of experimental and calculated data):

% Inhibition =

$$k_1[\text{cytochrome } c^{3+}] / (k_1[\text{cytochrome } c^{3+}] + k_2[\text{DMPO}]) \quad (3)$$

Chromium trioxalate is a membrane-impermeable spin-trap-broadening agent that broadens EPR signals located outside membrane-surrounded compartments [23,24]. Addition of

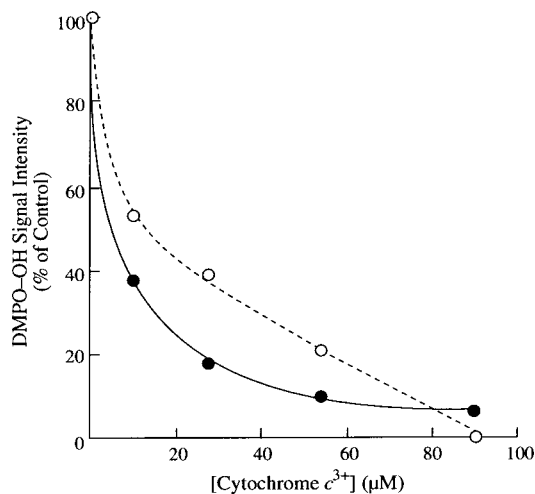


Figure 4 Inhibitory effect of cytochrome *c* on DMPO spin adduct generated by mitoplasts

Assay conditions were as for Figure 2(B) in the presence of varying amounts of ferricytochrome *c*. ○, Experimental data; ●, calculated data according to eqn. (3).

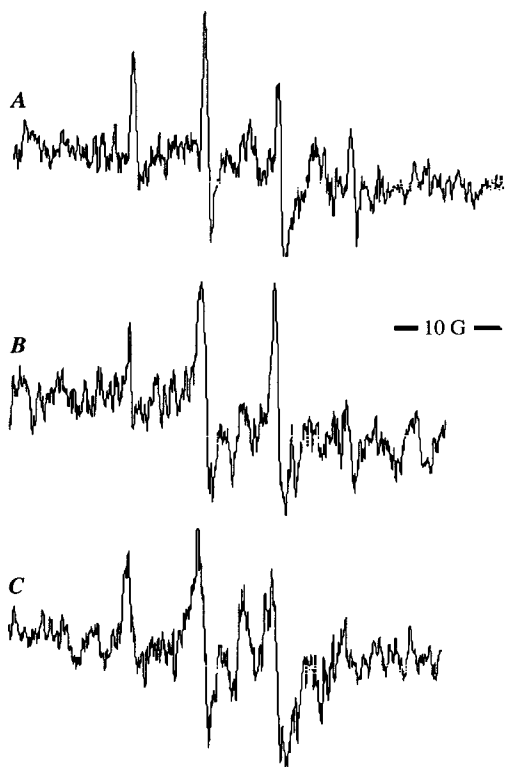


Figure 5 Effect of chromium oxalate on the DMPO-OH signal generated by antimycin-treated mitoplasts

Assay conditions were as for Figure 2(B) in the absence (A) and presence of 2.5 mM (B) and 5 mM (C) chromium trioxalate.

chromium trioxalate to antimycin-treated mitoplasts led to dose-dependent broadening of the DMPO-OH signal (Figure 5).

The observed inhibition of DMPO-OH by both membrane-impermeable cytochrome *c* and chromium trioxalate indicates that a portion of the DMPO-OH signal occurred in the inter-

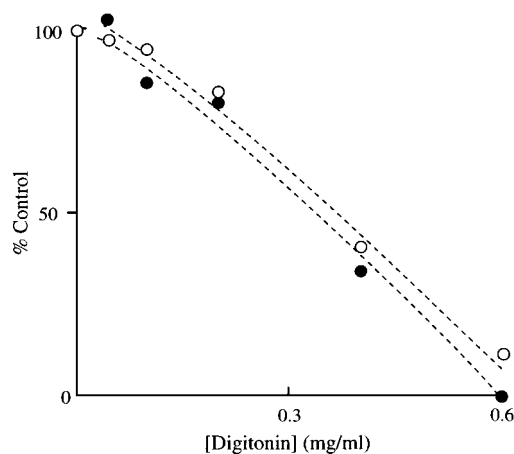


Figure 6 Effect of digitonin on superoxide production and respiration in mitoplasts

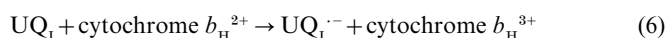
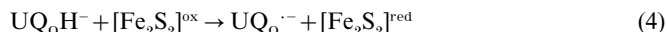
Evaluation of the effects of digitonin on the intensity of the DMPO spin-adduct signal (●) was performed as in Figure 2(A) in the presence of varying amounts of digitonin. State-3 respiration (○) was measured as described in the Materials and methods section in the presence of 2.5 μ M cytochrome *c*.

membrane space, thereby indicating that $O_2^{\cdot-}$ was vectorially released into this compartment. However, it may be argued that $O_2^{\cdot-}$ might originate from a small fraction of broken mitoplasts in the preparation. This possibility was examined by assessing the effect of digitonin on the EPR signal intensity obtained from mitoplasts. If broken mitoplasts were responsible for $O_2^{\cdot-}$ production, the further treatment of mitoplasts with digitonin would result in a higher EPR signal intensity. Digitonin treatment resulted in a dose-dependent decrease in the DMPO-OH signal (Figure 6) that correlated well with loss of respiration; these findings further support the notion that broken mitoplasts were not the cause of $O_2^{\cdot-}$ release in the intermembrane space.

Effect of electron-transfer inhibitors on superoxide anion production by mitoplasts

To elucidate the location in the electron-transport chain responsible for $O_2^{\cdot-}$ formation and release into the intermembrane space, the effect of various inhibitors was examined (Figure 7). Neither rotenone nor thenoyltrifluoroacetone (TTFA) generated an EPR signal unless antimycin was also added (results not shown), strengthening the notion that complexes I and II were not responsible for $O_2^{\cdot-}$ formation. A decrease in EPR signal intensity was observed in antimycin-treated mitoplasts in the presence of rotenone or TTFA. The simultaneous addition of rotenone and TTFA to antimycin-treated mitoplasts, which completely inhibits electron transport, led to a complete inhibition of the DMPO-OH signal, confirming that a fully functional electron-transport chain was necessary for $O_2^{\cdot-}$ formation.

Myxothiazol is a complex-III inhibitor that binds at the UQ_o site of the UQ pool, thereby blocking electron transfer from ubiquinol (UQ_oH_2 or its monoanionic form, Q_oH^-) to iron-sulphur clusters (eqn. 4) and to cytochrome b_L (eqn. 5). Antimycin binds to the UQ_I site, blocking electron transfer from haem b_H to UQ_I (eqn. 6) [25]:



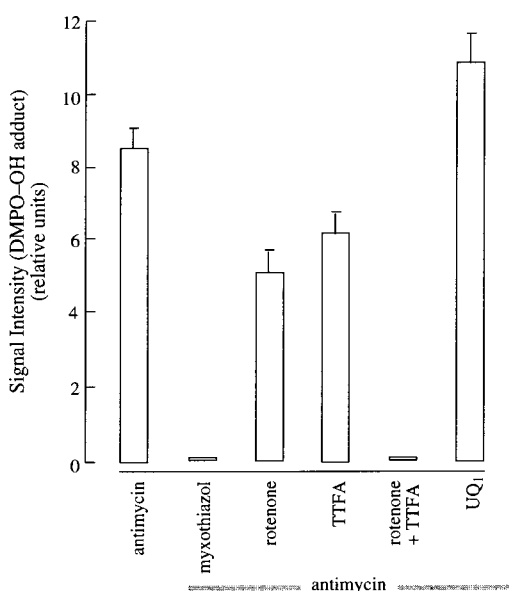
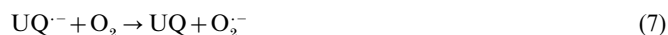


Figure 7 Effect of electron-transfer inhibitors and UQ₁ on spin-adduct signal intensity

Assay conditions were as for Figure 2(A) in the presence of different electron-transfer inhibitors: antimycin (1 μ g/mg of protein), myxothiazol (1 μ M), TTFA (20 μ M) and rotenone (2 μ M). UQ₁ concentration was 50 μ M.

where UQ₁^{•-} and UQ₀^{•-} indicate ubisemiquinone in the inner and outer UQ pools, respectively. Co-treatment of mitoplasts with antimycin and myxothiazol caused a complete loss of the DMPO-OH signal (Figure 7) in agreement with an expected inhibition of ubisemiquinone formation (eqns. 4–6) and the ensuing ubisemiquinone autoxidation (eqn. 7) [26,27]:



The addition of UQ₁ to mitoplasts resulted in an expanded UQ pool and, accordingly, a higher production of O₂^{•-} (Figure 7). This effect, reported previously with submitochondrial particles, requires electron transfer from complex I or II to the electron acceptor (UQ₁; eqn. 8) followed by its autoxidation (eqn. 7).



DISCUSSION

Mitoplasts, devoid of the outer-mitochondrial-membrane barrier, offer a highly fortuitous model for assessing the vectoriality of O₂^{•-} release taking into consideration the occurrence of an inner (UQ₁) and outer (UQ₀) pool of UQ, facing the matrix and intermembrane space, respectively. This study, carried out with mitoplasts (the functional integrity of which was similar to coupled mitochondria), showed that O₂^{•-}, detected by EPR as the corresponding spin adduct, was partly released into the mitochondrial intermembrane space. This view is supported by the effect of membrane-impermeable molecules on the spin-adduct signal: (i) abrogation of the EPR signal by Cu,Zn-superoxide dismutase (Figure 2C); (ii) decrease in the signal intensity by a mechanism involving competition between ferricytochrome *c* and the spin trap (Figure 4) and (iii) broadening of the EPR signal by chromium oxalate (Figure 5). These effects may not be ascribed to broken mitoplasts in the preparation caused by digitonin treatment (Figure 6).

The Q-cycle [28] within complex III involves ubiquinol oxidation and UQ reduction at the outer (UQ₀) and inner (UQ₁) UQ sites, respectively. Ubiquinol oxidation at the UQ₀ site requires bifurcation of two electrons: the first electron transfer (encompassed in the UQ₀H₂ → UQ₀^{•-} redox transition) is to the iron–sulphur centres (eqn. 4) and cytochrome *c*₁; this electron transfer is inhibited by myxothiazol. The second electron (encompassed in the UQ₀^{•-} → UQ₀ redox transition) is transferred to cytochrome *b*_L (eqn. 5) and to the inner UQ site (UQ₁) through cytochrome *b*_H (eqn. 6). Antimycin inhibits the latter electron transfer [9,29,30].

The selective site of action of mitochondrial electron-transport-chain inhibitors, such as antimycin and myxothiazol, strengthens the notion that autoxidation of UQ₀^{•-} is a source of O₂^{•-} production released into the intermembrane space. Antimycin has been shown experimentally to increase the steady-state levels of UQ₀^{•-} while completely inhibiting UQ₁^{•-} formation [29]. Conversely, myxothiazol was reported to have no effect on UQ₁^{•-} levels while it inhibits the formation of UQ₀^{•-} [29]. The observations that antimycin treatment was required for O₂^{•-} production in mitoplasts, while myxothiazol treatment inhibited O₂^{•-} production completely, suggest an important role for UQ₀^{•-} in O₂^{•-} production and its subsequent release into the intermembrane space. The data in this study do not rule out O₂^{•-} formation on the matrix side of the inner membrane and its release into the matrix; this view is supported experimentally by work carried out with submitochondrial particles [2].

Given the low transport of O₂^{•-} across membranes, it is reasonable to hypothesize that autoxidation of UQ₁^{•-} would result in O₂^{•-} being vectorially released into the matrix, whereas O₂^{•-} formed upon autoxidation of UQ₀^{•-} would have a greater probability of being released into the intermembrane space. Regardless of the site of release of O₂^{•-}, this species is generally considered membrane-impermeable [31], except in the protonated perhydroxyl radical form (HO₂[•]; eqn. 9), which represents a small fraction of the O₂^{•-} pool at physiological pH [32]:



Because HO₂[•] can cross membranes [31], it can be argued that some O₂^{•-} observed in the intermembrane space may originate from the matrix. However, due to the high levels of Mn-superoxide dismutase ($\approx 10^{-5}$ M), only 1.5×10^{-3} % of O₂^{•-}/HO₂[•] formed in the matrix may be expected to diffuse into the intermembrane space [33]. Thus it is unlikely that the mitochondrial matrix contributes significantly to the steady-state levels of O₂^{•-} in the intermembrane space.

H₂O₂ diffusing out of isolated mitochondria is assumed to represent the fraction of O₂^{•-} disproportionated by Mn-superoxide dismutase and escaping reduction by matrix glutathione peroxidase. Based on this study (and the occurrence of a Cu,Zn-superoxide dismutase in the intermembrane space [15a]), it may be inferred that part of the mitochondrial H₂O₂ may also originate from the intermembrane space. In fact, several factors favour the notion of the intermembrane space as a source of H₂O₂ diffusing from the mitochondria. First, based on fractionation experiments, the classic glutathione peroxidase has been found to reside only in the mitochondrial matrix [34], whereas a phospholipid hydroperoxide glutathione peroxidase is believed to be localized in the inner membrane and contact junctions between the inner and outer membranes [35,36]. Overall, the intermembrane space appears to possess a less-efficient peroxidase activity than the mitochondrial matrix. Second, due to mitochondrial membrane topology, the probability of H₂O₂ generated in the matrix reaching the cytosol is lower than that of H₂O₂

produced in the intermembrane space. The inner mitochondrial membrane acts as a barrier to decrease H_2O_2 diffusion, thereby increasing the efficiency of glutathione peroxidase [37]; conversely, the outer mitochondrial membrane, being porous, has no effect on H_2O_2 diffusion. Because the intermembrane space lacks any barriers limiting H_2O_2 diffusion and contains a low GSH-dependent peroxidase activity, H_2O_2 generated in this space probably diffuses rapidly into the cytoplasm. The observation that antimycin (that increases steady-state levels of UQ_0^-) increases H_2O_2 production by isolated mitochondria lends further support to the intermembrane space as a site of production of H_2O_2 .

Release of O_2^- towards the intermembrane space has implications for estimations of mitochondrial steady-state levels of H_2O_2 , especially those based on steady-state approximations involving an equilibrium between the formation and removal of H_2O_2 (eqn. 10) [38]:

$$+d[\text{H}_2\text{O}_2]/dt = -d[\text{H}_2\text{O}_2]/dt \quad (10)$$

Because glutathione peroxidase activity in the intermembrane space differs drastically from that in the matrix, such estimations carry a degree of inaccuracy, the extent of which depends on the actual amount of O_2^- released into the intermembrane space. Until the levels of O_2^- , Cu,Zn-superoxide dismutase and glutathione peroxidase are quantified in the intermembrane space, steady-state estimates of H_2O_2 cannot be assessed accurately in isolated mitochondria. Furthermore, a quantitative approach and calculation of steady-state levels of O_2^- in the intermembrane space are required to comprehend the physiological importance of this phenomenon. Similarly, steady-state estimates of mitochondrial O_2^- production that have been made using O_2^- measurements of submitochondrial particles [38] should be redefined as matrix O_2^- steady-state levels.

We are thankful to Dr Fernando Antunes for valuable discussions. This research was supported by National Institutes of Health grant 1R01-AG16718.

REFERENCES

- Chance, B., Sies, H. and Boveris, A. (1979) Hydroperoxide metabolism in mammalian organs. *Physiol. Rev.* **59**, 527–605
- Boveris, A. and Cadenas, E. (1975) Mitochondrial production of superoxide anions and its relationship to the antimycin-insensitive respiration. *FEBS Lett.* **54**, 311–314
- Dionisi, O., Galeotti, T., Terranova, T. and Azzi, A. (1975) Superoxide radicals and hydrogen peroxide formation in mitochondria from normal and neoplastic tissues. *Biochim. Biophys. Acta* **403**, 292–301
- Boveris, A., Cadenas, E. and Stoppani, A. O. M. (1976) Role of ubiquinone in the mitochondrial generation of hydrogen peroxide. *Biochem. J.* **156**, 435–444
- Cadenas, E., Boveris, A., Ragan, C. I. and Stoppani, A. O. M. (1977) Production of superoxide radicals and hydrogen peroxide by NADH-ubiquinone reductase and ubiquinol-cytochrome *c* reductase from beef-heart mitochondria. *Arch. Biochem. Biophys.* **180**, 248–257
- Boveris, A., Oshino, N. and Chance, B. (1972) The cellular production of hydrogen peroxide. *Biochem. J.* **128**, 617–630
- Turrens, J. F. and Boveris, A. (1980) Generation of superoxide anion by the NADH dehydrogenase of bovine heart mitochondria. *Biochem. J.* **191**, 421–427
- Tyler, D. D. (1975) Polarographic assay and intracellular distribution of superoxide dismutase in rat liver. *Biochem. J.* **147**, 493–504
- Brandt, U. (1996) Bifurcated ubihydroquinone oxidation in the cytochrome *bc1* complex by proton-gated charge transfer. *FEBS Lett.* **387**, 1–6
- Sharp, R. E., Moser, C. C., Gibney, B. R. and Dutton, P. L. (1999) Primary steps in the energy conversion reaction of the cytochrome *bc1* complex Qo site. *J. Bioenerg. Biomembr.* **31**, 225–233
- Butler, J., Koppenol, W. and Margoliash, E. (1982) Kinetics and mechanism of the reduction of ferricytochrome *c* by the superoxide anion. *J. Biol. Chem.* **257**, 10747–10750
- Weisiger, R. A. and Fridovich, I. (1973) Superoxide dismutase. Organelle specificity. *J. Biol. Chem.* **248**, 4793–4796
- Jackson, C., Dench, J., Moore, A. L., Halliwell, B., Foyer, C. H. and Hall, D. O. (1978) Subcellular localisation and identification of superoxide dismutase in leaves of higher plants. *Eur. J. Biochem.* **91**, 339–344
- Peeters-Joris, C., Vandevoorde, A.-M. and Baudhuin, P. (1975) Subcellular localization of superoxide dismutase in rat liver. *Biochem. J.* **150**, 31–39
- Geller, B. L. and Winge, D. R. (1982) Rat liver Cu,Zn-superoxide dismutase. Subcellular location in lysosomes. *J. Biol. Chem.* **257**, 8945–8952
- Fridovich, I. (2000) Mitochondrial Cu,Zn superoxide dismutase revisited. In *International Congress on Oxidants and Antioxidants in Biology*, March 1–4, 2000, Santa Barbara, CA, Book of Abstracts, p. 82
- Pedersen, P. L., Greenawalt, J. W., Reynafarje, B., Hulliher, J., Decker, G. L., Soper, J. W. and Bustamante, E. (1978) Preparation and characterization of mitochondria and submitochondrial particles of rat liver and liver-derived tissues. *Methods Cell Biol.* **20**, 411–481
- Gardner, P. R. and White, C. W. (1995) Application of the aconitase method to the assay of superoxide in the mitochondrial matrices of cultured cells: effects of oxygen, redox cycling agent, TNF- α , IL-1, LPS and inhibitors of respiration. In *The Oxygen Paradox* (Davies, K. J. A. and Ursini, F., eds), pp. 33–50, Cleup University Press, Padova
- Ernster, L. and Schatz, G. (1981) Mitochondria: a historical review. *J. Cell Biol.* **91**, 227s–255s
- Hoppel, C. L., Kerner, J., Turkaly, P., Turkaly, J. and Tandler, B. (1998) The malonyl-CoA-sensitive form of carnitine palmitoyltransferase is not localized exclusively in the outer membrane of rat liver mitochondria. *J. Biol. Chem.* **273**, 23495–23503
- Finkelstein, E., Rosen, G. M. and Rauckman, E. J. (1980) Spin trapping. Kinetics of the reaction of superoxide and hydroxyl radicals with nitrones. *J. Am. Chem. Soc.* **102**, 4994–4999
- Belkin, S., Mehlhorn, R. J., Hideg, K., Hankovsky, O. and Packer, L. (1987) Reduction and destruction rates of nitroxide spin probes. *Arch. Biochem. Biophys.* **256**, 232–243
- Quintanilha, A. T. and Packer, L. (1977) Surface localization of sites of reduction of nitroxide spin-labeled molecules in mitochondria. *Proc. Natl. Acad. Sci. U.S.A.* **74**, 570–574
- Berg, S. P. and Nesbitt, D. M. (1979) Chromium oxalate: a new spin label broadening agent for use with thylakoids. *Biochim. Biophys. Acta.* **548**, 608–615
- Lai, C. S., Froncisz, W. and Hopwood, L. E. (1987) An evaluation of paramagnetic broadening agents for spin probe studies of intact mammalian cells. *Biophys. J.* **52**, 625–628
- von Jagow, G. and Link, T. A. (1986) Use of specific inhibitors on the mitochondrial *bc1* complex. *Methods Enzymol.* **126**, 253–271
- Turrens, J. F., Alexandre, A. and Lehninger, A. L. (1985) Ubisemiquinone is the electron donor for superoxide formation by complex III of heart mitochondria. *Arch. Biochem. Biophys.* **237**, 408–414
- Ksenzenko, M., Konstantinov, A. A., Khomutov, G. B., Tikhonov, A. N. and Ruuge, E. K. (1983) Effect of electron transfer inhibitors on superoxide generation in the cytochrome *bc1* site of the mitochondrial respiratory chain. *FEBS Lett.* **155**, 19–24
- Mitchell, P. (1976) Possible molecular mechanisms of the protonmotive function of cytochrome systems. *J. Theor. Biol.* **62**, 327–367
- de Vries, S. (1986) The pathway of electron transfer in the dimeric QH₂: cytochrome *c* oxidoreductase. *J. Bioenerg. Biomembr.* **18**, 196–224
- Jünemann, S., Heathcote, P. and Rich, R. R. (1998) On the mechanism of quinol oxidation in the *bc1* complex. *J. Biol. Chem.* **273**, 21603–21607
- Gus'kova, R. A., Ivanov, I., Akhobadze, V. V. and Rubin, A. R. (1984) Permeability of bilayer lipid membranes for superoxide (O_2^-) radicals. *Biochim. Biophys. Acta* **778**, 579–583
- Sawyer, D. T. and Valentine, J. S. (1981) How super is superoxide? *Acc. Chem. Res.* **14**, 393–400
- Antunes, F., Salvador, A., Marinho, H. S., Alves, R. and Pinto, R. E. (1996) Lipid peroxidation in mitochondrial inner membranes. I. An integrative kinetic model. *Free Radical Biol. Med.* **21**, 917–943
- Green, R. C. and O'Brien, P. J. (1970) The cellular localisation of glutathione peroxidase and its release from mitochondria during swelling. *Biochim. Biophys. Acta* **197**, 31–39
- Panfilii, E., Sandri, G. and Ernster, L. (1991) Distribution of glutathione peroxidases and glutathione reductase in rat brain mitochondria. *FEBS Lett.* **290**, 35–37
- Goedas, C., Sandri, G. and Panfilii, E. (1994) Distribution of phospholipid hydroperoxide glutathione peroxidase (PHGPx) in rat testis mitochondria. *Biochim. Biophys. Acta* **1191**, 147–150
- Antunes, F. and Cadenas, E. (2000) Estimation of H_2O_2 gradients across biomembranes. *FEBS Lett.* **475**, 121–126
- Boveris, A. and Cadenas, E. (1997) Cellular sources and steady-state levels of reactive oxygen species, in *Oxygen, Gene Expression and Cellular Function* (Mazzaro, D. and Clerch, L., eds), pp. 1–25, Marcel Dekker, New York